Critical sheet resistance and two-dimensional properties of $Bi_2Sr_2CuO_x$ thin films

Masumi Inoue, Hiroshi Matsushita, and Hisao Hayakawa
Department of Electronics, Nagoya University, Furo-cho, Chikusa-ku, Nagoya 464-01, Japan

Kazushige Ohbayashi
Research and Development Center, NGK Spark Plug Co., Ltd., 14-18 Takatsuji-cho, Mizuho-ku, Nagoya 467, Japan
(Received 12 September 1994)

Electrical properties of $Bi_2Sr_2CuO_x$ thin films prepared by the RF magnetron sputtering method have been investigated. By varying the Bi content in the film, the resistance of $Bi_2Sr_2CuO_x$ changed over a wide range. Samples with low resistance showed superconductivity with a zero-resistance critical temperature of about 5 K, and the temperature dependence of the resistance above the superconducting transition temperature was metallic. On the other hand, samples with high resistance did not show superconducting transition and the temperature dependence of the resistance was semiconductorlike. The critical value of the normal resistance per Cu-O sheet for the appearance of the superconductivity was found to be very close to the quantum resistance ($h/4e^2$). In the case of superconductive films, the power law of current-voltage characteristics ($V \propto I^\alpha$) was observed and the temperature dependence of the exponent α showed the universal jump, which suggested the dissipation at the superconducting transition due to the Kosterlitz-Thouless (KT) transition. The temperatrure dependence of the resistance also supported the KT transition. The fluctuation effect above the mean-field BCS transition temperature was interpreted by the 2D Aslamazov-Larkin theory. In the case of insulating films, their behavior was examined by several mechanisms. The Anderson localization could be responsible for the $R_\square$-T characteristics of the sample of which sheet resistance was just above the critical resistance in the low-temperature region. The intriguing possibility of the KT transition of charges for high-resistance samples was also discussed.

I. INTRODUCTION

We have been trying to obtain high-quality $Bi_2Sr_2Ca_{n-1}Cu_nO_x$ (BSCCO) films by block-by-block sputtering.[1-5] In the case of 2223 phase, we could obtain as-grown films with very smooth surface morphology and a zero-resistance critical temperature T_{czero} of 102 K,[4] which is the highest value of T_{czero} of as-grown 2223 phase films to our knowledge. In this process of raising T_{czero}, we found that it was very important to adjust the Bi content for the deposition of high-quality films. The electrical properties were seriously affected by the subtle control of the Bi content. In particular, the electrical properties of 2201 phase (BSCO) films changed from superconductor to insulator.

This behavior of BSCO films is similar to the superconductor-insulator transition observed in films of other materials. Such transition has been reported in a variety of systems (granular films,[6-9] homogeneous ultrathin films,[10-16] high-T_c films,[17-19] Josephson-junction arrays[20]) and the critical resistance is a universal value, approximately $h/(4e^2)$, independent of the material and the microscopic details.

Cuprate superconductors such as $YBa_2Cu_3O_x$ (YBCO) and BSCCO are anisotropic materials and two-dimensional (2D) characteristics have been observed. The Kosterlitz-Thouless (KT)-type behavior reflects the 2D aspect of the sample. The appearance of the resistance just above the zero resistance critical temperature T_{czero} have been explained by the KT transition theory.[21] In metallic superconductors, this behavior was observed for various systems including ultrathin films,[22] granular films,[23,24] and Josephson-junction arrays.[25,26] After the discovery of oxide superconductors, the KT transition theory was also applied to the explanation of their properties[27-40] and some works were for single crystals, which may reflect the 2D characteristics of these materials.

The excess conductivity also reflects the dimensionality. Many works have been carried out and 2D behavior,[41-48] 3D behavior,[49] and 2D-3D crossover[50-52] have been reported. Though BSCO is also a member of such cuprate superconductors, its critical temperature T_c is rather low and its properties have been investigated less than other members with higher T_c.

In this paper we report the superconductor-insulator transition of BSCO films by the subtle control of the Bi content. We continue with a discussion of the electrical properties of the obtained films. In particular, their two-dimensional properties will be highlighted.

II. SAMPLE PREPARATION

We have prepared BSCCO and BSCO thin films of high quality *in situ* by the multitarget RF magnetron sputtering method,[1-4] and also confirmed this method to be applicable to the preparation of BSCCO/BSCO superlattices.[5] Two targets of 3 in diameter were used for the

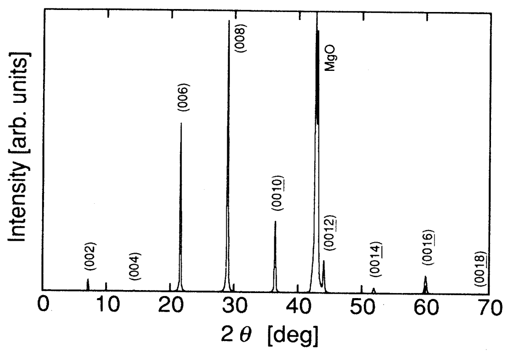

FIG. 1. X-ray-diffraction pattern of a BSCO film prepared at input power 2 of 10 W.

deposition of BSCO films. The compositions of targets 1 and 2 were $Bi_{2.0}Sr_{2.0}Cu_{1.0}O_x$ (single-phase calsined powder) and Bi (5*N*, metal), respectively. Target 2 (Bi) was used in order to make the adjustment of the composition in the film easy. This target is essential for the deposition of high-quality BSCO films because the properties of the BSCO films are very sensitive to the Bi content, as will be mentioned later. The Bi content in the film was controlled by the input power to target 2. The films were grown on MgO(100) substrates at the substrate temperature of 760 °C. The substrate was fastened to the substrate table which rotated at 24 rpm, and run periodically just along the circumference which joins the center of the targets. The sputtering gas was a mixture of argon and oxygen ($Ar:O_2=4:1$) and the total pressure was 1.0 Pa. The input powers to targets 1 and 2, which we denote by input power 1 and input power 2 hereafter, were 42 and 8–14 W, respectively. The deposition time was 2 h, which corresponds to the thickness of 730 Å. After the deposition, air was introduced into the chamber to atmospheric pressure, and the substrate was cooled. In order to determine the deposition rate and the optimum sputtering conditions, BSCCO films were prepared by the alternate deposition of Bi-Sr-Cu-O blocks and Ca-Cu-O blocks, which was reported previously. In this case, target 3 ($Ca_{1.0}Cu_{1.0}O_x$, sintered) was used for the deposition of the Ca-Cu-O block, and targets 1 and 2 for the Bi-Sr-Cu-O block.

The obtained BSCO films were of good crystallinity and well oriented, and had very smooth surface morphology. Figure 1 shows the x-ray-diffraction pattern of the BSCO film prepared at input power 2 of 10 W. The film was a single phase and showed a well-defined *c*-axis orientation. Other films prepared in the range of input power 2 mentioned above showed almost the same patterns. The lattice constant *c* was 24.60 Å and its deviation was within 0.1%.

III. RESISTANCE MEASUREMENTS

We need precise measurements of the resistance for the discussion below. Therefore, we first considered the method of the resistance measurement. Here we compare two kinds of four-probe methods. Method 1 was carried out using the electrode arrangement shown in Fig. 2: two line electrodes carrying the current and two small electrodes for voltage measurement. Electrical contacts were made with silver paste covering the edge of the film. This arrangement is close to the definition of the sheet resistance. This method may include some errors because the current flow lines are not completely parallel near both current electrodes. However, these errors will be small and the obtained resistivity will be fairly precise because the voltage electrodes are very small. In this method, the resistance of the sample R_3 is obtained readily from the relationship between the measuring current and the voltage drop. R_3 can be translated to the sheet resistance per Cu-O plane $R_\square$ by

$$R_\square = R_2 \frac{W}{L} = R_3 n \frac{W}{L} , \qquad (1)$$

where R_2 is the resistance of a Cu-O plane, W the width of the sample, L the length of the sample and n the number of the Cu-O planes in the sample.

Method 2 was the van der Pauw technique,[53] which is of great practical importance and gives a 3D resistivity of a flat sample of arbitrary shape. Four separate small contacts were placed at the corners of the sample. In this method, the 3D resistivity of the sample ρ_3 is obtained. The resistance of the sample measured by method 1 is expressed using ρ_3 by

$$R_3 = \rho_3 \frac{L}{Wdn} , \qquad (2)$$

where d is the distance between two adjacent Cu-O planes. Substituting Eq. (2) into Eq. (1), ρ_3 can be translated to $R_\square$ by

$$R_\square = \frac{1}{d} \rho_3 . \qquad (3)$$

In order to compare these two methods, measurements were carried out using two pieces divided from the same sample. One piece was measured by method 1 and the other by method 2. $R_\square$ values obtained for some samples by methods 1 and 2 are compared in Table I. As seen in the table, values obtained by the two methods showed a little difference, however, the ratios of the two values

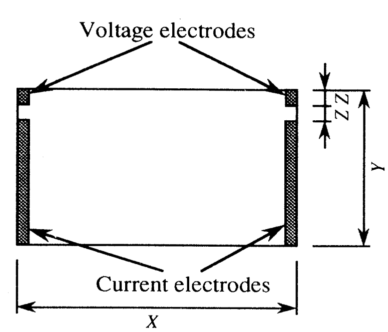

FIG. 2. Electrode arrangement for the measurement of the resistance by method 1. Usually $X=5$ mm, $Y=3$ mm, and $Z=0.3$ mm.

TABLE I. Comparison of the sheet resistance values obtained by methods 1 and 2 for three samples. $R_{\square 1}$ and $R_{\square 2}$ are the sheet resistances measured by method 1 and method 2, respectively.

Sample No.	$R_{\square 1}$ [Ω]	$R_{\square 2}$ [Ω]	$R_{\square 2}/R_{\square 1}$
1	2228	2889	1.296
2	4980	6270	1.269
3	5680	7361	1.296

were almost the same for all the samples. Therefore, clear relationship was recognized between the two methods. Hereafter we use the $R_\square$ value measured by method 2 as the sheet resistance.

IV. RESULTS AND DISCUSSION

A. Bi content and *I-V* characteristics

Electrical properties of the BSCO films are very sensitive to the Bi content. Figure 3 shows the dependence of current-voltage (*I-V*) characteristics on input power 2. Such variation was also observed when Bi_2O_3 was used as target 2, instead of Bi metal, and the Bi content increased with increasing input power 2. The Bi content for samples in Fig. 3 was not measured, however, it can be inferred from the results obtained using the Bi_2O_3 target, and estimated to be 1.8 to 2.1 (assuming that the Sr content is 2.0) for samples *A* to *G*. At low Bi content the sheet resistance was very high and increased as the temperature decreased like semiconductors. $R_\square$ decreased with increasing Bi content and the *I-V* curve changed from semiconductorlike one to metallic one. At around the optimum content the *I-V* curve showed superconducting transition and zero-resistance temperature T_{czero} above the liquid-He temperature. Further increase in the Bi content raised $R_\square$ again and the zero resistance was not observed above 4.2 K. Previously,[2] we reported that T_{czero} and the Bi mean valence of the 2223 phase changed with Bi content. Clear correlation between T_{czero} and the Bi mean valence was observed and the data for 2223 and 2212 phase films and the 2212/2201 superlattices could be plotted on an identical curve. These results suggest that the Bi-O layer works as a hole-providing layer to the Cu-O plane and determines the superconducting properties. Therefore we consider that the variation of the *I-V* curves of BSCO films in Fig. 3 also reflects the change in the hole density in the Cu-O plane with the Bi content.

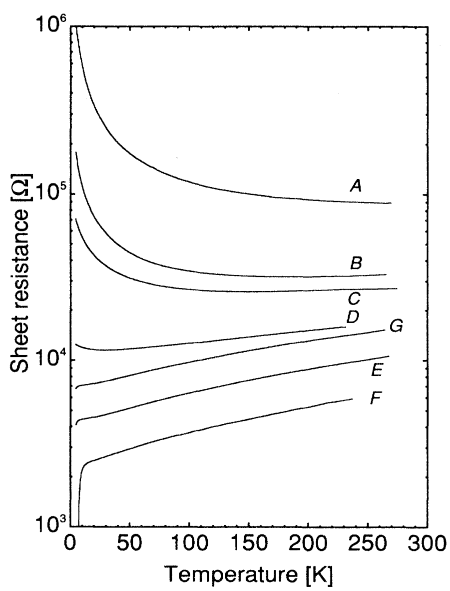

FIG. 3. Temperature dependence of the sheet resistance of $Bi_2Sr_2CuO_x$ and its variation with the Bi content. The Bi content increases with increasing input power to the Bi target (*A*:8 W, *B*:9 W, *C*:9.3 W, *D*:10 W, *E*:10 W, *F*:10.2 W, and *G*:11 W).

Here we notice that there is a critical sheet resistance R_c which divide the samples into two groups: samples which show the superconducting transition onset and those which do not show the onset. This critical value is defined as the sheet resistance just above the superconducting transition temperature where the slope of the $R_\square$-T curve is 0. Figure 4 shows the sheet resistance dependence of $d(\ln R_\square)/dT$ at 10 K, and R_c is estimated at $7-9\times10^3$ Ω. In order to evaluate R_c more precisely, we take the effect of the degraded layers just above the substrate into account. The electrical properties of such layers are not good because of the lattice mismatch between the substrate and the film, the interactive diffusion at the BSCO/MgO interface, etc. This degraded part includes 2–3 unit cells, which is inferred from the number of buffer layers (2201 phase) necessary for the growth of high-quality films of the 2223 phase. Namely 4–6 Cu-O layers make a less contribution to the electric conduction and should be excluded in the calculation. This means that the sheet resistance reported here should be lower than the measured value by about 8%. Therefore, the critical resistance is estimated at 7 ± 1 kΩ. This value is quite close to the quantum resistance $R_Q=h/(4e^2)=6.5$ kΩ. Such transition from superconductor to semiconductor (or insulator) near R_Q has also been reported in

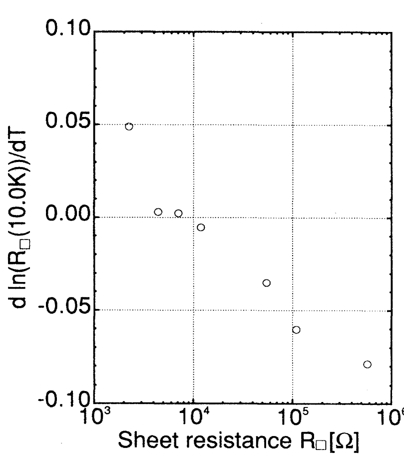

FIG. 4. Dependence of $d(\ln R_\square)/dT$ on the sheet resistance $R_\square$ at 10 K. Samples with positive value of $d(\ln R_\square)/dT$, i.e., positive slope in $R_\square-T$ characteristics at 10 K, showed the onset of superconducting transition above 4.2 K.

various systems of metals and oxide superconductors.[6–20] In particular, similar behavior of the sheet resistance per Cu-O layer was also observed for $Nd_{2-x}Ce_xCuO_4$ thin films.[18,19] Thus the characteristics shown in Fig. 3 are considered to represent universal properties and suggest that the Cu-O plane plays an important role in electric conduction in BSCO.

B. Superconducting film

Low-resistance samples showed superconducting transition and T_{czero} was observed above 5 K. The temperature dependence of the sheet resistance of such superconducting film (sample F in Fig. 3) is shown in Fig. 5. Here we consider this superconducting transition. The appearance of the resistance in two-dimensional superconducting systems have been explained by the Kosterlitz-Thouless (KT) transition theory. We try to apply this theory to our BSCO films. In the KT transition theory, vortices and antivortices are bound in pairs in the low-temperature region, however, as the temperature increases the vortex-antivortex pairs start to dissociate and the resistance appears because of the vortex motion in the current. The temperature dependence of this resistance R is expressed as

$$\frac{R}{R_n} = a \exp\left\{-2\left[b\frac{T_{co}-T}{T-T_{\mathrm{KT}}}\right]^{1/2}\right\}, \tag{4}$$

where T is the temperature, R_n the normal resistance, T_{co} the mean-field BCS transition temperature, T_{KT} the KT transition temperature, and a and b are constants of order unity. In Fig. 6 we show a plot of $\ln(R_\square/R_n)$ vs $[(T_{co}-T)/(T-T_{\mathrm{KT}})]^{1/2}$ for the transition temperature region. This plot gave a straight line when $T_{\mathrm{KT}}=5.5$ K and $T_{co}=7.3$ K. Constants a and b are 4.8 and 3.9, respectively, which are of order unity. These fitted values are reasonable and therefore Fig. 6 suggests the possibility of the KT transition.

Other evidences for the KT transition are the power law[54] in the voltage-current (V-I) characteristics, i.e., $V \propto I^\alpha$, and the universal jump[55] of the exponent $\alpha = 1+\pi K_R$ at T_{KT}, where K_R is the renormalized stiffness constant. Figure 7 shows the V-I characteristics of the superconducting BSCO film on a log-log plot around T_{czero}. Strong nonlinearity was observed below T_{czero} and it became weaker as the temperature increased. At 7.29 K, the dependence was linear. In the small current limit, a straight line was obtained at each temperature. Thus the power law $V \propto I^\alpha$ was confirmed. In the KT transition theory, the exponent α of the power law decreases with increasing temperature and jumps from 3 to 1 at T_{KT}, or πK_R jumps from 2 to 0 at T_{KT}. The temperature dependence of πK_R of our superconducting BSCO film is shown in Fig. 8. A jump can be observed and T_{KT} obtained from this figure is 5.6 K, which is nearly equal to the value obtained from Fig. 6. Thus, the appearance of the resistance above T_{czero} can be attributed

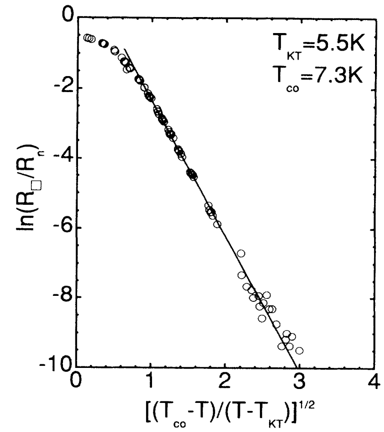

FIG. 6. Temperature dependence of the sheet resistance in $\ln(R_\square/R_n)$ vs $[(T_{co}-T)/(T-T_{\mathrm{KT}})]^{1/2}$ plot for the same sample as in Fig. 5 (sample F) with $T_{\mathrm{KT}}=5.5$ K and $T_{co}=7.3$ K.

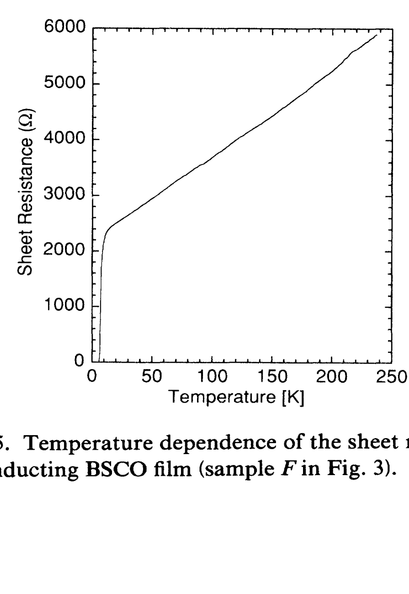

FIG. 5. Temperature dependence of the sheet resistance for a superconducting BSCO film (sample F in Fig. 3).

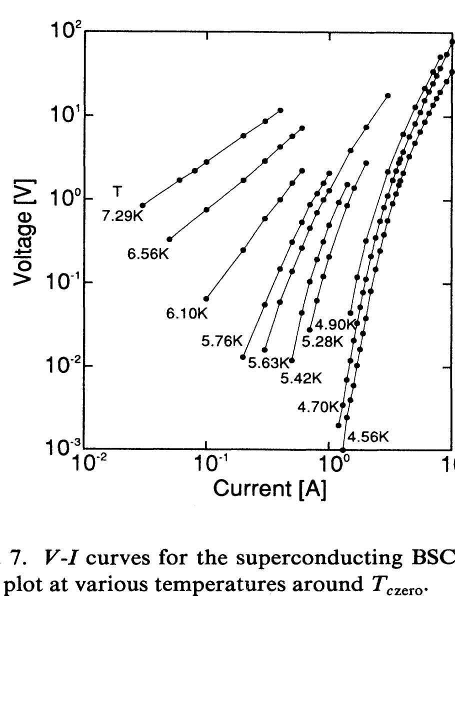

FIG. 7. V-I curves for the superconducting BSCO film on a log-log plot at various temperatures around T_{czero}.

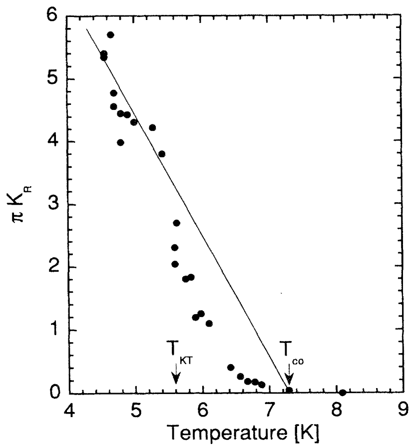

FIG. 8. Temperature dependence of the renormalized stiffness constant for the superconducting BSCO film. A straight line is drawn to fit the data below T_{KT} and the intersection of this line and $\pi K_R = 0$ determines T_{co}.

to the KT transition.

T_{co} corresponds to the critical temperature below which Cooper pairs are formed, however, Cooper pairs also appear by fluctuation even above T_{co}, which causes the decrease in the resistance. Such effect of the fluctuation have been explained by the Aslamazov-Larkin (AL) theory[56,57] and the Maki-Thompson (MT) theory.[58,59] We calculated the $R_\square$-T characteristics using AL and MT terms and compared them with the measured curve. Consequently we found that the 2D AL term produced the most favorable result. The sheet resistance $R_\square$ is expressed as

$$R_\square(T) = \left[\frac{1}{AT+B} + \frac{e^2}{16h} t^{-1} \right]^{-1}, \quad (5)$$

where e is the electric charge of an electron, A and B are constants, and $t = (T - T_{co})/T_{co}$. Figure 9 shows the $R_\square$-T characteristic in the temperature region of the superconducting transition together with the theoretical curves for the KT transition and the fluctuation above T_{co}. Characteristic temperatures used for the calculation are $T_{KT} = 5.5$ K and $T_{co} = 7.3$ K.

From the above discussion, we can divide the $R_\square$-T characteristics of the superconducting BSCO film into four regions. In region 1 ($T < T_{KT}$), vortex-antivortex pairs are formed and the film shows zero resistance. In region 2 (about T_{KT}), unpaired vortices start to appear and the film shows finite resistance. In region 3 (about T_{co}), the two-dimensional fluctuation of superconductivity reduces the resistance, and in region 4 ($T \gg T_{co}$), the normal resistance with linear temperature dependence is observed.

C. Insulating film

We discuss the electrical properties of high-resistance films here. The resistance of these films increased with decreasing temperature and was considered to enter into the insulating state near 0 K. There are various conduc-

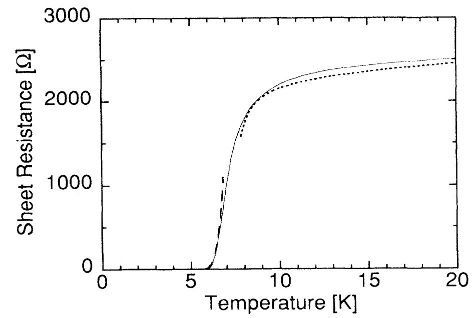

FIG. 9. Temperature dependence of the sheet resistance of the same sample as shown in Fig. 5 (sample F) in the temperature range of the superconducting transition (solid line) together with the fittings for the KT transition (broken line) and the fluctuation above T_{co} (dotted line).

tion mechanisms for semiconducting and insulating materials. First, we think of the energy band model where the conductivity σ shows the $\exp(-E_g/k_B T)$ dependence, i.e., $\log\sigma$ is proportional to $1/T$. However, straight lines were not obtained in the temperature dependence of the sheet conductance $G_\square$ in $\log G_\square$ vs $1/T$ plot for samples A, B, C, and D, which showed semiconducting behavior in the low-temperature region. Figure 10(a) shows the result for sample B as an example. Therefore we can rule out this mechanism.

The transition from superconductor to insulator is often attributed to some kind of localization. Next, we consider the variable range hopping model. In this model, a localized electron hops to the next site where the hopping probability is maximum, and the dimensionality appears in the temperature dependence of σ which is ex-

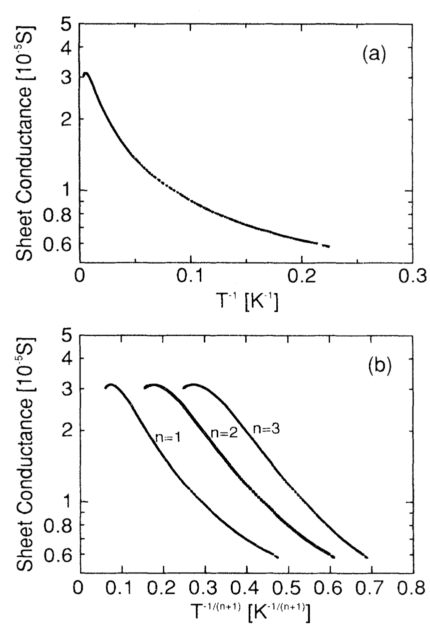

FIG. 10. Temperature dependence of the sheet conductance (a) in $\log G_\square$ vs $1/T$ plot and (b) in $\log G_\square$ vs $T^{-1/(n+1)}$ plot for sample B.

pressed as

$$\sigma=\sigma_0\exp(-AT^{-1/(n+1)}) , \quad (6)$$

where n is the dimensionality. The temperature dependence of the sheet conductance of samples A to D in the $\log G_\square$ vs $T^{-1/(n+1)}$ plot did not give straight lines for $n=1$ and 2. Curves for $n=3$ seemed most likely, however, they were not sufficient to suggest this mechanism. The result for sample B is shown in Fig. 10(b) as an example.

The quantum interference effect in disordered potential structure causes the Anderson localization.[60–62] In two-dimensional system, σ in the weak-localization regime can be expressed as

$$\sigma=\sigma_0+\sigma_a p \ln T , \quad (7)$$

where p is the power of T in the temperature dependence of the relaxation time ($\tau \propto T^{-p}$). Figure 11 shows the $G_\square$ vs $\ln T$ plot for samples A to D. Among these samples, sample D shows $\ln T$ dependence of $G_\square$, which suggests the possibility of the Anderson localization in the low-temperature region. However, samples A, B, and C do not show the $\ln T$ dependence. Therefore, the Anderson localization mechanism is ruled out for these samples, and they are considered to be in the stronger localization regime, though the mechanism is not clear as discussed above.

Here we consider another possibility of the insulating behavior. Fazio *et al.* presented charge-vortex duality in the KT transition in Josephson-junction arrays[63] and the competition between the charge and the vortex unbinding.[64] We have confirmed the KT transition for vortices in our BSCO films above. Here we examine the possibility of the KT transition of charges in this system. The correlation length ξ in the KT transition shows the following temperature dependence:

$$\xi \propto \exp(b'/\sqrt{T/T'_{KT}-1}) , \quad (8)$$

where b' is a constant of order unity and T'_{KT} is the KT transition temperature of charges. $G_\square$ is proportional to the density of the charged particle, and it is proportional to ξ^{-2}. Thus $G_\square$ just above T'_{KT} can be expressed as

$$G_\square=G_0\exp(-2b'/\sqrt{T/T'_{KT}-1}) , \quad (9)$$

where G_0 is a constant.

Figure 12 shows the temperature dependence of $G_\square$ in the $\log G_\square$ vs $(T/T'_{KT}-1)^{-1/2}$ plot for sample A below 10 K. The plot gave almost a straight line. A little deviation from the straight line between 4.5 and 6 K can be attributed to the fluctuation of the heating rate in the measurement of the R-T characteristics. Since the fitted value of T'_{KT} is very small and $T \gg T'_{KT}$, the exponent in Eq. (9) is $-2b'/\sqrt{T/T'_{KT}-1} \approx -2b'\sqrt{T'_{KT}}/\sqrt{T}$. Thus b' and T'_{KT} are hard to be determined independently. We obtained T'_{KT} assuming the value of b' to be a number of order unity. The fitted value of T'_{KT} is 0.11 K for $b'=6$ and 0.23 K for $b'=4$. On the other hand, for samples B, C, and D, the $\log G_\square$ vs $(T/T'_{KT}-1)^{-1/2}$ plot showed a slightly-curved line not to give a straight line even between 10 and 4.2 K, while we cannot deny the possibility of $(T/T'_{KT}-1)^{-1/2}$ dependence of σ below 4.2 K now.

The T'_{KT} values of samples B to D may be too low to explain the data above 4.2 K. We obtained T'_{KT} tentatively also for samples B to D approximating the data between 10 and 4.2 K by a straight line in the $\log G_\square$ vs $(T/T'_{KT}-1)^{-1/2}$ plot. The T'_{KT} values for samples A to D are shown in Fig. 13 as a function of the sheet conduc-

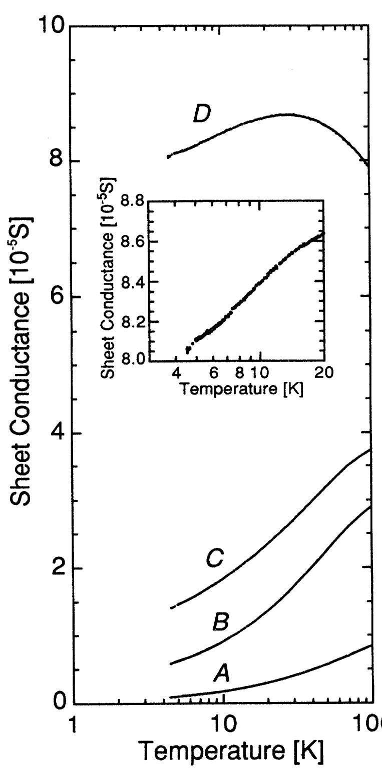

FIG. 11. Temperature dependence of the sheet conductance in $G_\square$ vs $\log T$ plot for samples A, B, C, and D. The inset shows another plot with magnified coordinates for sample D.

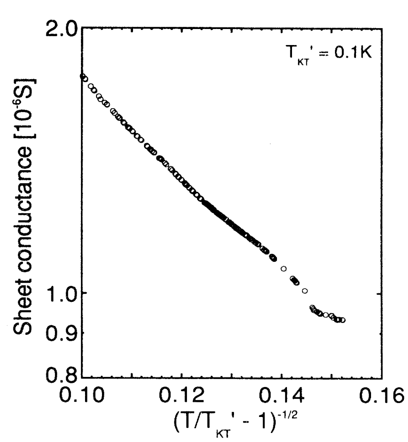

FIG. 12. Temperature dependence of the sheet conductance in $\log G_\square$ vs $(T/T'_{KT}-1)^{-1/2}$ plot for sample A with $T'_{KT}=0.1$ K.

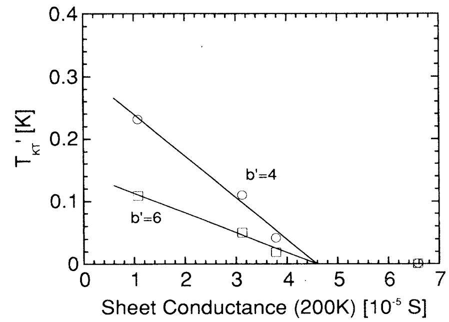

FIG. 13. T'_{KT} values obtained for samples *A*, *B*, *C*, and *D* as a function of the sheet conductance at 200 K. Open circles and open squares are for $b'=4$ and $b'=6$, respectively.

tance at 200 K where the sheet resistance is almost constant in the $R_\square$-T characteristics (Fig. 3). Obviously T'_{KT} decreases with increasing sheet conductance and becomes 0 at 4.6×10^{-5} S, i.e., at the sheet resistance of 22 kΩ, regardless of the value of b'. The KT transition theory for Josephson junction arrays predicts that T'_{KT} decreases with decreasing tunneling resistance and reduces to 0 at the tunneling resistance of 14 kΩ,[65] which agrees with the results of our system qualitatively. Thus, though these data above 4.2 K appear not to be sufficient to give positive support to this mechanism, its possibility at very low temperature cannot be denied now.

However, there are some questions. The first one is whether the theory for Josephson-junction arrays can be applied to our system or not. Second, it is necessary that positive and negative charges are bound in pairs in the above theory and then what is the counter charge that forms a pair with a hole in the Cu-O plane? If there are not such appropriate counter charges, the Wigner crystal[66,67] may be taken into account. The melting of the Wigner crystal lattice can also be explained by the KT transition of dislocation.[68] However, in the case of the electron lattice on the superfluid ^{4}He film, the sheet density of the electrons should be about 10^9 cm^{-2} or less. The carrier density in the Cu-O plane of BSCO is estimated to be higher by several orders[69,70] and it is not clear how such system should be treated. Therefore, we confine ourselves here to propose only the possibility of the KT transition of charges.

V. CONCLUSIONS

Electrical properties of BSCO thin films prepared by the RF magnetron sputtering method were investigated. By varying the Bi content in the film, the resistance of BSCO changed over a wide range. Films with low resistance showed superconductivity with a zero-resistance critical temperature of about 5 K, and the temperature dependence of the resistance above the superconducting transition temperature was metallic. On the other hand, films with high resistance did not show superconducting transition and the temperature dependence of the resistance was semiconductorlike. The critical value of the normal resistance per Cu-O sheet for the appearance of the superconductivity R_c was found to be very close to the quantum resistance ($h/4e^2$). In the case of superconductive films, the power law of current-voltage characteristics ($V\propto I^\alpha$) was observed and the temperature dependence of α showed the "universal jump," which suggested the dissipation at the superconducting transition due to Kosterlitz-Thouless transition. The temperature dependence of the resistance also supported the KT transition. The fluctuation effect above T_{co} was interpreted by the 2D Aslamazov-Larkin theory.

On the other hand, the $R_\square$-T characteristics of the insulating films were examined by several mechanisms. The Anderson localization could be responsible for the $R_\square$-T characteristics of the sample of which sheet resistance was just above R_c at the low-temperature region. The intriguing possibility of the KT transition of charges for high-resistance samples was also discussed. More experiments and discussion from various viewpoints will be required for the further interpretation of the behavior of these insulating films.

ACKNOWLEDGMENT

The authors wish to acknowledge Professor S. Maekawa for valuable discussions.

[1]K. Ohbayashi, M. Anma, Y. Takai, and H. Hayakawa, Jpn. J. Appl. Phys. **29**, L2049 (1990).
[2]K. Ohbayashi, K. Yoshida, M. Anma, Y. Takai, and H. Hayakawa, Jpn. J. Appl. Phys. **31**, L953 (1992).
[3]K. Ohbayashi, H. Matsushita, K. Yoshida, M. Anma, Y. Takai, and H. Hayakawa, IEEE Trans. Appl. Supercond. **3**, 1547 (1993).
[4]K. Ohbayashi, T. Ohtsuki, H. Matsushita, H. Nishiwaki, Y. Takai, and H. Hayakawa, Appl. Phys. Lett. **64**, 369 (1994).
[5]M. Inoue, K. Yoshida, K. Ohbayashi, Y. Takai, and H. Hayakawa, Physica C **200**, 403 (1992).
[6]B. G. Orr, H. M. Jaeger, A. M. Goldman, and C. G. Kuper, Phys. Rev. Lett. **56**, 378 (1986).
[7]B. G. Orr, H. M. Jaeger, and A. M. Goldman, Phys. Rev. B **32**, 7586 (1985).
[8]S. Kobayashi and F. Komori, J. Phys. Soc. Jpn. **57**, 1884 (1988).
[9]A. Gerber, J. Phys. Condens. Matter. **2**, 8161 (1990).
[10]H. M. Jaeger, D. B. Haviland, A. M. Goldman, and B. G. Orr, Phys. Rev. B **34**, 4920 (1986).
[11]N. Nishida, S. Okuma, and A. Asamitsu, Physica B **169**, 487 (1991).
[12]D. B. Haviland, Y. Liu, and A. M. Goldman, Phys. Rev. Lett. **62**, 2180 (1989).
[13]D. B. Haviland, Y. Liu, B. Nease, and A. M. Goldman, Physica B **165&166**, 1457 (1990).
[14]A. F. Hebard and M. A. Paalanen, Phys. Rev. B **30**, 4063 (1984).
[15]A. F. Hebard and M. A. Paalanen, Phys. Rev. Lett. **65**, 927 (1990).
[16]S. J. Lee and J. B. Ketterson, Phys. Rev. Lett. **64**, 3078 (1990).
[17]T. Wang, K. M. Beauchamp, D. D. Berkley, B. R. Johnson,

J.-X. Liu, J. Zhang, and A. M. Goldman, Phys. Rev. B **43**, 8623 (1991).
[18]S. Tanda, M. Honma, and T. Nakayama, Phys. Rev. B **43**, 8725 (1991).
[19]S. Tanda, S. Ozeki, M. Honma, A. Ohi, and T. Nakayama, Physica C **185-189**, 1323 (1991).
[20]L. J. Geerligs and J. E. Mooij, Physica B **152**, 212 (1988).
[21]J. M. Kosterlitz and D. J. Thouless, J. Phys. C **6**, 1181 (1973).
[22]A. M. Kadin, K. Epstein, and A. M. Goldman, Phys. Rev. B **27**, 6691 (1983).
[23]A. F. Hebard and A. T. Fiory, Phys. Rev. Lett. **44**, 291 (1980).
[24]S. A. Wolf, D. U. Gubser, W. W. Fuller, J. C. Garland, and R. S. Newrock, Phys. Rev. Lett. **47**, 1071 (1981).
[25]D. J. Resnick, J. C. Garland, J. T. Boyd, S. Shoemaker, and R. S. Newrock, Phys. Rev. Lett. **47**, 1542 (1981).
[26]D. W. Abraham, C. J. Lobb, M. Tinkham, and T. M. Klapwijk, Phys. Rev. B **26**, 5268 (1982).
[27]P. C. E. Stamp, L. Forro, and C. Ayache, Phys. Rev. B **38**, 2847 (1988).
[28]N.-C. Yeh and C. C. Tsuei, Phys. Rev. B **39**, 9708 (1989).
[29]Q. Y. Ying and H. S. Kwok, Phys. Rev. B **42**, 2242 (1990).
[30]V. A. Gasparov, Physica C **178**, 449 (1991).
[31]A. T. Fiory, A. F. Hebard, P. M. Mankiewich, and R. E. Howard, Phys. Rev. Lett. **61**, 1419 (1988).
[32]J. C. Culbertson, U. Strom, S. A. Wolf, P. Skeath, and W. K. Burns, Phys. Rev. B **39**, 12 359 (1989).
[33]M. Rasolt, T. Edis, and Z. Tešanović, Phys. Rev. Lett. **66**, 2927 (1991).
[34]H. R. Kerchner, D. K. Christen, C. E. Klabunde, J. O. Thomson, Y. R. Sun, and J. R. Thompson, Physica C **198**, 75 (1992).
[35]Y. Matsuda, S. Komiyama, T. Terashima, K. Shimura, and Y. Bando, Phys. Rev. Lett. **69**, 3228 (1992).
[36]D. P. Norton and D. H. Lowndes, Phys. Rev. B **48**, 6460 (1993).
[37]M. Ban, T. Ichiguchi, and T. Onogi, Phys. Rev. B **40**, 4419 (1989).
[38]T. Onogi, T. Ichiguchi, and T. Aida, Solid State Commun. **69**, 991 (1989).
[39]S. Martin. A. T. Fiory, R. M. Fleming, G. P. Espinosa, and A. S. Cooper, Phys. Rev. Lett. **62**, 677 (1989).
[40]D. H. Kim, A. M. Goldman, J. H. Kang, and R. T. Kampwirth, Phys. Rev. B **40**, 8834 (1989).
[41]M. Ausloos and Ch. Laurent, Phys. Rev. B **37**, 611 (1988).
[42]S. Ravi and V. Seshu Bai, Solid State Commun. **83**, 117 (1992).
[43]M.-O. Mun, S.-I. Lee, S.-H. Suck Salk, H. J. Shin, and M. K. Joo, Phys. Rev. B **48**, 6703 (1993).
[44]F. Vidal, J. A. Veira, J. Maza, J. J. Ponte, F. García-Alvarado, E. Morán, J. Amador, C. Cascales, A. Castro, M. T. Casais, and I. Rasines, Physica C **156**, 807 (1988).
[45]G. Balestrino, M. Marinelli, E. Milani, L. Reggiani, R. Vaglio, and A. A. Varlamov, Phys. Rev. B **46**, 14 919 (1992).
[46]D. H. Kim, A. M. Goldman, J. H. Kang, K. E. Gray, and R. T. Kampwirth, Phys. Rev. B **39**, 12 275 (1989).
[47]F. Vidal, J. A. Veria, J. Maza, J. J. Ponte, J. Amador, C. Cascales, M. T. Casais, and I. Rasines, Physica C **156**, 165 (1988).
[48]J. A. Veria, J. Maza, and F. Vidal, Phys. Lett. A **131**, 310 (1988).
[49]P. P. Freitas, C. C. Tsuei, and T. S. Plaskett, Phys. Rev. B **36**, 833 (1987).
[50]B. Oh, K. Char, A. D. Kent, M. Nastio, M. R. Beasley, T. H. Geballe, R. H. Hammond, A. Kapitulnik, and J. M. Graybeal, Phys. Rev. B **37**, 7861 (1988).
[51]N. P. Ong, Z. Z. Wang, S. Hagen, T. W. Jing, and J. Hovarth, Physica C **153-155**, 1072 (1988).
[52]P. Mandal, A. Poddar, A. N. Das, B. Ghosh, and P. Choudhury, Physica C **169**, 43 (1990).
[53]L. J. van der Pauw, Philips Res. Rep. **13**, 1 (1958).
[54]B. I. Halperin and D. R. Nelson, J. Low Temp. Phys. **36**, 599 (1979).
[55]D. R. Nelson and J. M. Kosterlitz, Phys. Rev. B **39**, 1201 (1977).
[56]L. G. Aslamazov and A. I. Larkin, Phys. Lett. A **26**, 238 (1968).
[57]L. G. Aslamazov and A. I. Larkin, Fiz. Tverd. Tela (Leningrad) **10**, 1104 (1968) [Sov. Phys. Solid State **10**, 875 (1968)].
[58]R. S. Thompson, Phys. Rev. B **1**, 327 (1970).
[59]For a review, see W. J. Skocpol and M. Tinkham, Rep. Prog. Phys. **38**, 1049 (1975).
[60]P. W. Anderson, Phys. Rev. **109**, 1492 (1958).
[61]P. W. Anderson, Rev. Mod. Phys. **50**, 191 (1978).
[62]N. F. Mott, Rev. Mod. Phys. **50**, 203 (1978).
[63]R. Fazio, A. van Otterlo, G. Schön, H. S. J. van der Zant, and J. E. Mooij, Helv. Phys. Acta **65**, 228 (1992).
[64]R. Fazio and G. Schön, Phys. Rev. B **43**, 5307 (1991).
[65]J. E. Mooij, B. J. van Wees, L. J. Geerligs, M. Peters, R. Fazi, and G. Schön, Phys. Rev. Lett. **65**, 645 (1990).
[66]E. P. Winger, Phys. Rev. **46**, 1002 (1934).
[67]C. C. Grimes and G. Adams, Phys. Rev. Lett. **42**, 795 (1979).
[68]G. Deville, A. Valdes, E. Y. Andrei, and F. I. B. Williams, Phys. Rev. Lett. **53**, 588 (1984).
[69]D. R. Harshman and A. P. Mills, Jr., Phys. Rev. B **45**, 10 684 (1992).
[70]Y. Idemoto and K. Fueki, Physica C **190**, 502 (1992).